

RESEARCH

Open Access



# The diagnostic efficacy of diffusion tensor imaging in children with chronic kidney disease: correlation with histopathology and serum biomarkers

Manar Mansour<sup>1</sup>, Ali H. Elmokadem<sup>1\*</sup> , Ahmed A. Abd Elrazek<sup>1</sup>, Ayman Hammad<sup>2</sup>, Marwa R. Abd-Almoaty<sup>2</sup>, Khadiga M. Ali<sup>3</sup>, Dina Abdalla Ibrahim<sup>3</sup> and Tarek Elsayed Barakat<sup>2</sup>

## Abstract

**Background** Children with chronic kidney disease (CKD) usually present with disease impact on growth besides cardiovascular problems that not only impact the patient's health during childhood but also affect their adult life. We aimed to identify the diagnostic role of diffusion tensor imaging (DTI) in CKD in pediatric using its metrics: apparent diffusion coefficient (ADC) and fraction anisotropy (FA).

**Results** This prospective study was performed on thirty-five CKD patients (16 girls, 19 boys; mean age  $12.3 \pm 2.6$  years) and 19 sex- and age-matched controls. Both groups underwent renal DTI and renal function tests. Based on renal biopsy, patients with CKD were further categorized into sclerotic CKD ( $n = 25$ ) and non-sclerotic CKD ( $n = 10$ ). Mean FA renal medulla/cortex in CKD ( $0.18 \pm 0.18$  and  $0.20 \pm 0.17$ ) was lower significantly ( $p = 0.001$ ) than volunteers' ( $0.31 \pm 0.19$ ,  $0.27 \pm 0.18$ ). The cutoff FA of renal medulla/cortex used for CKD diagnosis was 0.22 and 0.23 with AUC of 0.828, 0.838 and accuracy of 80.8%, 82.8%. Mean of renal medulla/cortex ADC in CKD ( $2.13 \pm 0.23$  and  $1.93 \pm 0.22 \times 10^{-3} \text{ mm}^2/\text{s}$ ) was higher significantly ( $p = 0.001$ ) than that of volunteers' ( $1.67 \pm 0.15$  and  $1.64 \pm 0.133 \times 10^{-3} \text{ mm}^2/\text{s}$ ). ADC cutoff value of renal medulla/cortex used for CKD diagnosis was 1.86 and  $1.74 \times 10^{-3} \text{ mm}^2/\text{s}$  with AUC of 0.827, 0.82, 0.827, and 0.911, and accuracy of 80.6%, 79.6%, 82.8%, and 84.2%. Renal medulla/cortex FA in sclerotic CKD was significantly different ( $p = 0.001$ ) from non-sclerotic CKD ( $0.25 \pm 0.07$  and  $0.26 \pm 0.08$ ). Cortical and medullary FA in CKD patients correlated with e-GFR ( $r = 0.363$ ,  $r = 0.317$ ) and serum creatinine ( $r = -0.467$ ,  $r = -0.383$ ).

**Conclusions** Renal cortical/medullary FA can assist in diagnosing pediatric CKD, predict sclerotic CKD, and correlate with some serum biomarkers.

**Keywords** Diffusion tensor imaging, MRI, Pediatric, Chronic kidney disease, Glomerulosclerosis

## Background

Chronic kidney disease (CKD) is a clinical condition in which a progressive loss of renal function occurs. The Kidney Disease Improving Global Outcomes (KDIGO) guidelines have defined CKD as kidney function or structure abnormalities lasting for more than three months that could cause implications to the health. Children with CKD usually present with disease impact on growth

\*Correspondence:

Ali H. Elmokadem  
mokadem83@yahoo.com

<sup>1</sup> Department of Radiology, Mansoura University, Mansoura, Egypt

<sup>2</sup> Department of Pediatrics, Mansoura University Children Hospital, Mansoura, Egypt

<sup>3</sup> Department of Pathology, Mansoura University, Mansoura, Egypt



© The Author(s) 2024. **Open Access** This article is licensed under a Creative Commons Attribution 4.0 International License, which permits use, sharing, adaptation, distribution and reproduction in any medium or format, as long as you give appropriate credit to the original author(s) and the source, provide a link to the Creative Commons licence, and indicate if changes were made. The images or other third party material in this article are included in the article's Creative Commons licence, unless indicated otherwise in a credit line to the material. If material is not included in the article's Creative Commons licence and your intended use is not permitted by statutory regulation or exceeds the permitted use, you will need to obtain permission directly from the copyright holder. To view a copy of this licence, visit <http://creativecommons.org/licenses/by/4.0/>.

besides cardiovascular problems, that not only impact the patient's health during childhood but also affect their adult life [1, 2]. Renal fibrosis refers to the deposition of the pathological matrix in the interstitial space, glomerular capillaries' walls, and around arterioles secondary to metabolic, toxic, immunological, and mechanical insults. Scarring of renal parenchyma can negatively impact renal function by progressive loss up to end-stage renal failure that entails permanent dialysis or renal transplantation. End-stage kidney disease manifests histologically as fibrotic lesions affecting different compartments; tubulointerstitial fibrosis, glomerulosclerosis, and vascular sclerosis. The histological pattern can predict and contribute to the functional demise of the kidney [3, 4].

Serum biomarkers as blood urea nitrogen level, serum creatinine, and estimated glomerular filtration rate (e-GFR) are helpful parameters for assessing renal function and grading the disease severity. Still, they cannot reflect morphological changes in the kidney. Ultrasonography, CT, and MR can provide anatomic images without functional information. Contrast media used in MRI and CT studies can induce systemic nephrogenic fibrosis and nephrotoxicity, respectively. Hence, this limits their use in patients with chronic kidney disease. Scintigraphy is a well-established imaging tool that merely assesses renal function by measuring glomerular filtration rate; however, it results in radiation exposure and has a lower spatial resolution. Evaluation of renal parenchymal microstructure is crucial to diagnose and monitor kidney diseases. It is now established by renal biopsy, which is an invasive procedure with hazardous side effects and sampling bias [5, 6].

Diffusion-weighted imaging (DWI) is a noninvasive imaging tool that depends on the diffusivity of water molecules within a tissue. It can give an idea about the structural changes of the tissue occurring in different pathologies in addition to its ability to quantitatively assess the magnitude of water diffusion [7–10]. Diffusion tensor imaging (DTI) is a powerful technique based on DWI, as DWI allows assessment of the water random motion and provides information about how the tissue cellular structures are aligned. It enables the analysis of anisotropic properties of the tissues by determining the principal directions of preferential water diffusion, which can be expressed quantitatively by DTI metrics: apparent diffusion coefficient (ADC) and fractional anisotropy (FA) [9–11]. DTI was used in the assessment of renal parenchyma in the normal population [12] and various renal disorders: renal allograft [13, 14], renal fibrosis [15, 16], glomerulonephritis [17], diffuse kidney parenchymal disease [18–20], lupus nephritis [21], and diabetes-induced nephropathy in humans [22] and rats [23]. This work aims to identify the diagnostic value of DTI in

pediatric CKD and detect the correlation between the DTI parameters, clinical and pathological stages of CKD disease.

## Methods

### Patients

Parents of enrolled children signed informed consent, and institutional review board approval was obtained. The study included 38 children prepared for renal biopsy due to chronic kidney disease with high serum creatinine levels and low GFR. All patients were diagnosed with chronic kidney disease based on Kidney Disease Improving Global Outcomes (KDIGO) guidelines [1]. Patients with chronic liver, blood disease, or neoplastic disease were excluded. Finally, the study group of 35 patients underwent conventional MR imaging and renal DTI. A control group of 19 children of matched age and sex were included in the study. The control group comprised children without a history of renal diseases who were referred to perform abdominal MRI to assess other pathologies rather than a renal disease and had normal renal function tests.

### Diffusion tensor imaging

MRI scans were done using a 1.5 Tesla scanner (Ingenia, Philips, Best, Netherlands). Subjects were scanned in the supine position, and two coils were applied; the anterior one, which is a phased-array torso surface coil (16-channel), and another posterior body coil within the table to obtain maximum image uniformity. To attain respiratory-triggered acquisition to reduce the respiratory motion-induced artifact, 5-mm coronal navigator slice was put on the dome of the liver. Conventional MR protocol was first done, including Axial T1-weighted images (TE/TR = 25/600 ms) and axial T2-weighted FSE sequence (TR/TE = 80/3200 ms). The following parameters were used: field of view (FOV) = 220 × 222 mm<sup>2</sup>, matrix = 92 × 88, gap interval = 0.5 mm, and slice thickness = 5 mm. Then, DTI was obtained using 32 direction, b value = 0 and 1000 s/mm<sup>2</sup>. Respiratory-gated, single-shot DTI—echo-planar imaging (DTI-EPI) was performed (TR/TE 3220/90 ms) with the following parameters: voxel dimensions = 2.54 × 2.43 × 2.5 mm<sup>3</sup>, data matrix = 92 × 88, slice thickness = 2.5 mm without gap, FOV = 220 × 222 mm<sup>2</sup>, and the scan duration = 7–8 min.

### Image analysis

Diffusion tensor imaging data were processed by a workstation with DTI functional tool software (Extended Philips MR Workspace 2.6.3.2). Two expert radiologists with ten and twenty years of experience in MR imaging performed the analysis. Both observers were not informed by patients' laboratory and clinical

data. Axial T1 and T2 were assessed to exclude any gross abnormalities. FA and ADC color maps were extracted. T2 images with distinctive cortico-medullary differentiation were applied directly to the opposing co-registered FA and ADC maps to measure the cortical and medullary FA and ADC accurately. Three regions of interest (ROI single-pixel seed) (Fig. 3) were placed in different regions in the cortex and medulla of both kidneys, approximately in the anterior, middle, and posterior regions away from the hilar vessels. The ADC and FA of different cortical and medullary regions were calculated. The mean values of both kidneys representing the renal FA and ADC for each subject were used for the statistical analysis (Fig. 1).

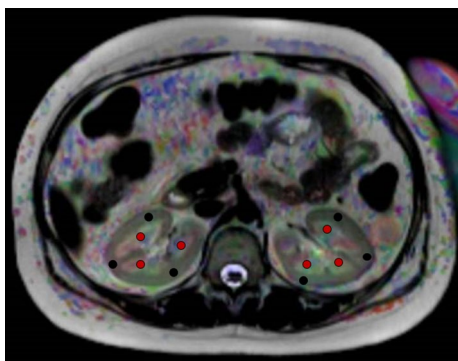


**Fig. 1** Region of interest localization. DTI color map of kidney shows the localization of ROI within the cortex/medulla of both kidneys in a child with CRPD

### Renal biopsy

Under sterilized conditions and local anesthesia, an ultrasound-guided biopsy was performed. Patients lied in prone or lateral decubitus position, and a 16-gauge core needle was used. Cores were sent for light and electron microscopy evaluation. Pathologists were asked to assess the histopathological pattern of CKD and categorize the study group into sclerotic (Fig. 2) and non-sclerotic renal disease (Fig. 3) based on the presence of glomerulosclerosis.

### Serum and urinary biomarkers

Serum creatinine was calculated by using COBAS INTEGRA 400 plus device. The Bedside Schwartz equation was used for estimating e-GFR from serum creatinine [24].

### Statistical analysis

Data were collected, revised, and sent for analysis using a statistical package for social science (SPSS, version 22.0. Armonk, NY: IBM Corp). Quantitative data were represented by the mean and standard deviation of the ADC, FA, e-GFR, and serum creatinine. Testing of the statistically significant difference was judged at (0.05) level. To compare between two groups, one sample student t test was used. The Chi-square test was used for comparison between more two groups. The optimal cutoff point utilizing the area under curve analysis (AUC), diagnostic capability, sensitivity, specificity, and accuracy of the cortical and medullary FA and ADC was performed using the receiver operating characteristic (ROC) analysis. It was used to differentiate between diseased and control groups and between the sclerotic and non-sclerotic

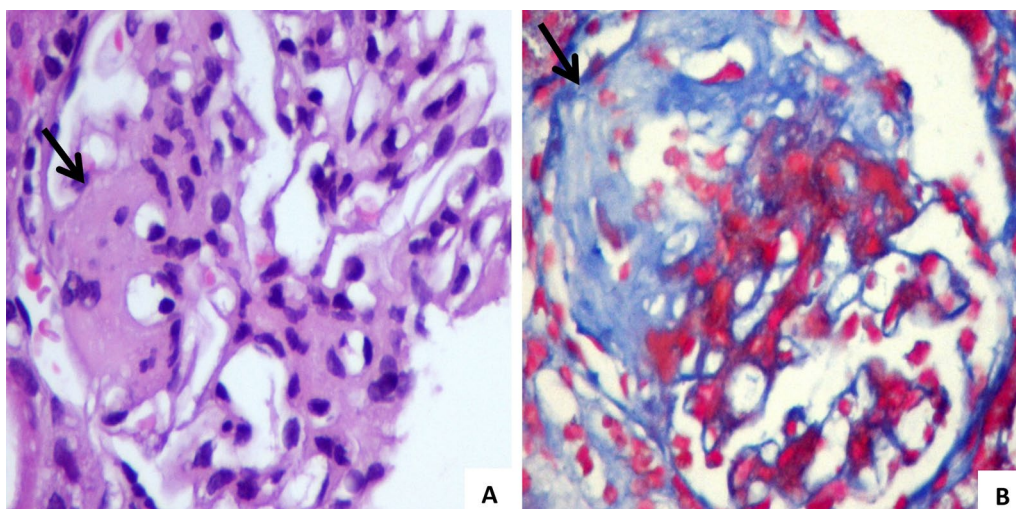


**Fig. 2** Focal segmental glomerulosclerosis (FSGS). **A** H&E stain shows focal mesangial sclerosis (Black arrow, magnification 400×) that was highlighted with Masson trichrome stain (**B**). Renal cortex FA was 0.17 and ADC was  $1.88 \times 10^{-3} \text{ mm}^2/\text{s}$ , FA for medulla was 0.15 and ADC was  $1.92 \times 10^{-3} \text{ mm}^2/\text{s}$



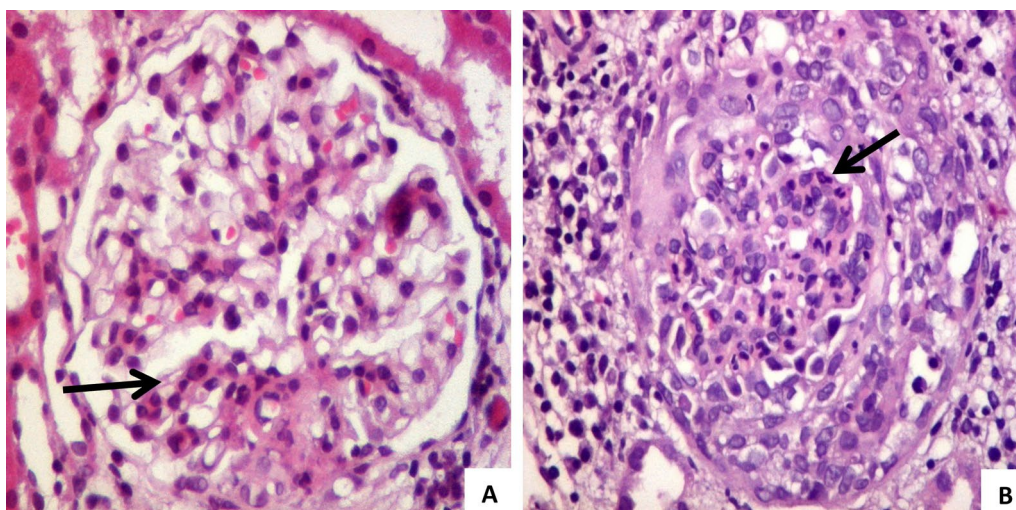


**Fig. 3** **A** Mesangioproliferative glomerulonephritis (MPGN) shows mild mesangial expansion with mild hypercellularity (case of lupus nephritis class II) (Black arrow) (H&E, magnification 400x). Renal cortex FA was 0.27 and ADC was  $2.25 \times 10^{-3} \text{ mm}^2/\text{s}$ , FA for medulla was 0.24 and ADC was  $2.09 \times 10^{-3} \text{ mm}^2/\text{s}$ . **B** Crescentic glomerulonephritis shows cellular crescents (Black arrow) with mesangial hypercellularity and neutrophilic infiltrate (H&E, magnification 400x). Renal cortex FA was 0.26 and ADC was  $2.21 \times 10^{-3} \text{ mm}^2/\text{s}$ , FA for medulla was also 0.25 and ADC was  $1.99 \times 10^{-3} \text{ mm}^2/\text{s}$

groups. Spearman’s rank-order correlation was used to determine the linear relationship’s direction and strength between renal parenchyma FA and ADC and laboratory parameters (e-GFR and serum creatinine). A Kappa agreement (GraphPad Software Inc. CA) was estimated by cross-tabulation for categorical variables with Kappa as follows (slight agreement from 0.01 to 0.20, fair agreement from 0.21 to 0.40, moderate agreement from 0.41 to 0.60, good agreement from 0.61 to 0.80, and perfect agreement from 0.81 to 0.99).

**Result**

The study group comprised 35 patients (19 boys, 16 girls with a mean age of  $12.23 \pm 2.79$  years), while the control group was composed of 19 children (10 boys and 9 girls; mean age,  $11.0 \pm 2.50$  years). Table 1 shows CKD patients’ age, sex, clinical, urinary biomarkers, serum, and DTI parameters versus the control group. All scans show a normal morphological appearance of both kidneys with no signal abnormalities. The etiology of CKD varied from obstructive uropathy, hypertension, hypoplastic or dysplastic kidneys, reflux nephropathy, focal segmental glomerulosclerosis, polycystic kidney disease, and juvenile-onset lupus erythematosus.

The mean renal medulla/cortex FA value of CKD patients ( $0.18 \pm 0.18$  and  $0.20 \pm 0.17$ ) was significantly lesser ( $p=0.001$ ) than that of the volunteers ( $0.31 \pm 0.19$ ,  $0.27 \pm 0.18$ ). The cutoff values of FA of the medulla/cortex used to diagnose CKD were 0.22 and 0.23 with AUC of 0.828, 0.838, and accuracy of 80.8%, 82.8% (Fig. 4a). The

**Table 1** Demographic, serum, and DTI parameters of CKD patients and controls

	CKD N=35	Control N=19	p value
<i>Demographic</i>			
Age (years)	12.2±2.7 (7–18)	11.0±2.5 (6–15)	0.23
Sex (M–F)	19/16	10/9	0.16
<i>Serum parameters</i>			
Serum creatinine (mg/dl)	1.41±0.267	0.89±0.22	<0.001*
e-GFR	47.6±7.12	73.2±16.5	<0.001*
<i>Diffusion parameters</i>			
Cortex: FA	0.20±0.07	0.27±0.08	<0.001*
ADC ( $\times 10^{-3} \text{ mm}^2/\text{s}$ )	1.98±0.23	1.65±0.13	<0.001*
Medulla: FA	0.18±0.08	0.31±0.09	<0.001*
ADC ( $\times 10^{-3} \text{ mm}^2/\text{s}$ )	2.03±0.23	1.68±0.16	<0.001*

Data presented as mean ± SD

\*Statistically significant

mean ADC value of the renal medulla/cortex of CKD patients ( $2.13 \pm 0.23$  and  $1.93 \pm 0.22 \times 10^{-3} \text{ mm}^2/\text{s}$ ) was significantly higher ( $p=0.001$ ) than that of the volunteers ( $1.67 \pm 0.15$  and  $1.64 \pm 0.133 \times 10^{-3} \text{ mm}^2/\text{s}$ ). The cutoff ADC values of the medulla/cortex used to diagnose CKD were 1.86 and  $1.74 \times 10^{-3} \text{ mm}^2/\text{s}$  with AUC of 0.827, 0.82, 0.827, and 0.911 and accuracy of 80.6%, 79.6%, 82.8%, and 84.2% (Fig. 4b).

Sclerosis was proved by histopathology in 25 out of 35 patients. The mean value of FA of renal medulla/

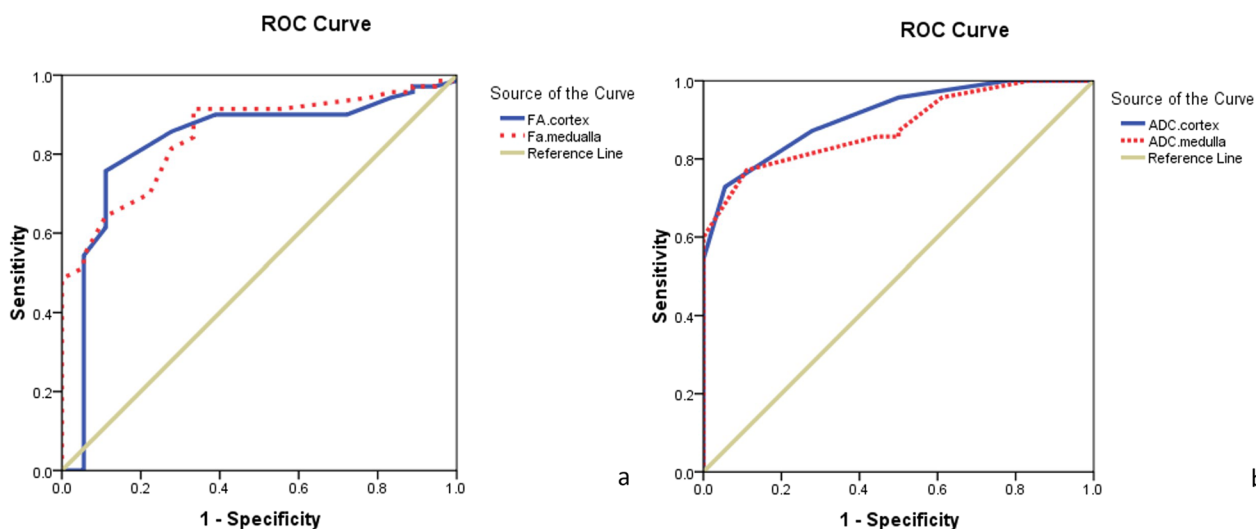


**Fig. 4** **A** ROC of FA. The cutoff values of FA of the cortex/medulla used to diagnose CKD were 0.23, 0.22, AUC is 0.828, 0.848, and accuracy is 82.9%, 80.7% respectively. **B** ROC of ADC. The cutoff values of ADC of the cortex/medulla used to diagnose CKD were 1.75,  $1.85 \times 10^{-3} \text{ mm}^2/\text{s}$ , AUC is 0.910, 0.81, and accuracy is 84.1%, 79.5% respectively

**Table 2** Mean FA & ADC cortex and medulla according to the presence of sclerosis

Sclerosis	P value		
	Present N=25	Absent N=10	
<i>DTI parameters</i>			
Cortex: FA	0.17 ± 0.05	0.26 ± 0.06	< 0.001*
ADC ( $\times 10^{-3} \text{ mm}^2/\text{s}$ )	1.98 ± 0.17	2.0 ± 0.349	0.813
Medulla: FA	0.16 ± 0.06	0.24 ± 0.08	< 0.001*
ADC ( $\times 10^{-3} \text{ mm}^2/\text{s}$ )	2.046 ± 0.2	1.99 ± 0.25	0.362

Data presented as mean ± SD (range)

\*Statistically significant

cortex in pathologically proven sclerotic CKD ( $0.16 \pm 0.06$ ,  $0.17 \pm 0.05$ ) was statistically lower ( $p=0.001$ ) than that of non-sclerotic CKD ( $0.25 \pm 0.07$ ,  $0.26 \pm 0.08$ ). The renal ADC of the renal medulla in pathologically proven sclerotic CKD ( $2.04 \pm 0.22 \times 10^{-3} \text{ mm}^2/\text{s}$ ) was higher ( $p=0.362$ ) than that of non-sclerotic CKD ( $1.99 \pm 0.25 \times 10^{-3} \text{ mm}^2/\text{s}$ ). Table 2 shows the DTI parameters of the sclerotic versus non-sclerotic group.

The mean renal cortex/medulla FA value of CKD patients negatively correlated with serum creatinine ( $r=-0.467$ ,  $p=0.001$ ,  $r=-0.383$ ,  $p=0.000$  respectively) and negatively correlated with e-GFR ( $r=0.363$ ,  $p=0.002$ ,  $r=0.317$ ,  $p=0.006$  respectively). The ADC of the renal cortex/medulla in patients with CKD showed insignificant correlation with e-GFR ( $r=-0.157$ ,  $p=0.193$ ,  $r=0.097$ ,  $p=0.425$  respectively) and serum creatinine ( $r=0.157$ ,  $p=0.193$ ,  $r=-0.115$ ,  $p=0.342$  respectively).

Figure 5 demonstrates the correlation between FA with serum creatinine and e-GFR.

The Kappa coefficient indicated good to excellent inter-observer agreement as regards the FA and ADC reading in renal cortex and medulla (Table 3).

### Discussion

In this study, the main finding was a significant difference between the cortical and medullary FA and ADC in CKD patients and the control group. Moreover, we found a significant difference between FA in patients with sclerotic CKD versus non-sclerotic CKD. A correlation was found between DTI and laboratory parameters, including serum creatinine and e-GFR.

The FA value represents the ability of diffusion tensor imaging to detect anisotropic diffusion. It is mainly related to the preferential direction of medullary molecular diffusion due to the radial orientation of the renal vessels and tubules, in addition to the contribution to microcirculation [19, 20]. In this study, the mean FA value of the renal cortex/medulla in patients with CKD is statistically reduced from that of a control group. This reduction in diffusion anisotropy is possibly caused by structural parenchymal changes in CKD, such as cellular infiltration, interstitial fibrosis, and tubular atrophy in various CKD. Medullary FA was a sensitive and accurate marker for the detection of CKD, which is coping with many authors who considered medullary FA as a marker for renal structural integrity alteration and a useful potential index for kidney disease diagnosis in children [25–27]. Additionally, Li et al. concluded that medullary

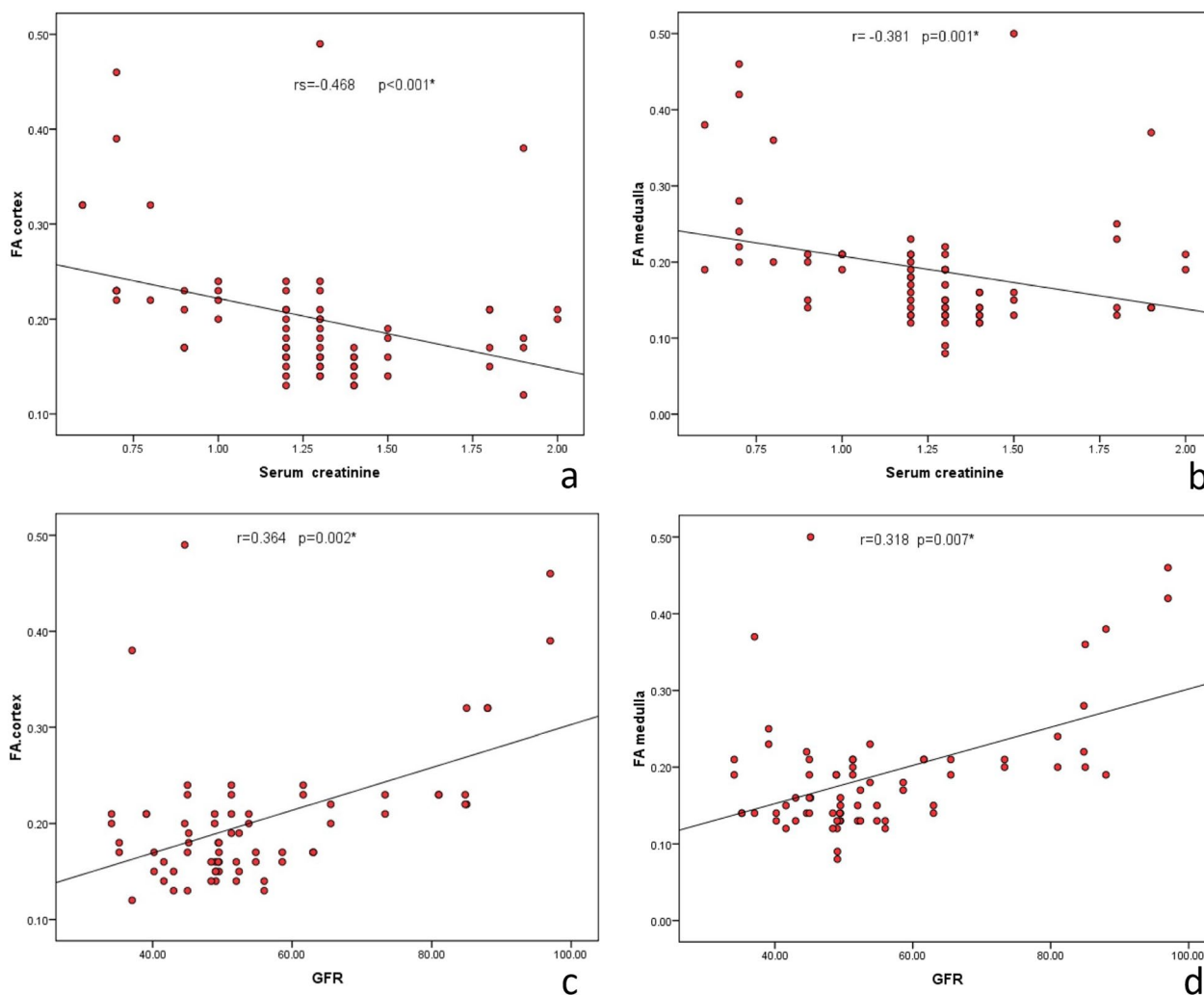


**Fig. 5** Scatter diagrams show correlation between FA of renal cortex/medulla, serum creatinine, and GFR

**Table 3** Inter-observer agreement for DTI parameters

		Intraclass correlation	95% CI	
			Lower level	Upper level
FA	Cortex	0.76	0.64	0.84
	Medulla	0.82	0.72	0.89
ADC	Cortex	0.73	0.58	0.82
	Medulla	0.92	0.78	0.98

FA is a noninvasive tool of assessing pediatric renal allograft health and correlates to several renal allograft histopathology scores [28].

Apparent diffusion coefficient or mean diffusivity quantifies cellular and membrane density where an increase in mean diffusivity indicates disease processes such as edema or necrosis. Whereas the FA is related to

the water molecule transport in the collecting tubules, the ADC is mainly influenced by perfusion [20]. Disrupted microcirculation and molecular diffusion by structural parenchymal changes influence the cortical and medullary perfusion and subsequently affect the ADC [18]. In this study, the ADC value of the renal cortex/medulla in patients with CKD is statistically higher than that of volunteers. There is a discrepancy regarding the relationship between ADC and CKD in the current literature. In agreement with our results, Ye et al. found that cortical and medullary ADC values showed a trend toward an increase in the diabetic group with early-stage kidney disease as compared to the control group [29]. Gaudio et al. found no significant difference for the cortical and medullary ADC values between the control and the CKD groups [19]. Contrary to our results, some studies reported that the ADC value was lower in the disease group than in control subjects [26–30]. Mao et al.

added that the ADC value is significantly lower in the medulla than the cortex for both patients and controls ( $p=0.01$ ) [31]. This discrepancy may be secondary to different parameters used for DTI, various hydration conditions of the patients, various disease duration, in addition to variable grades of active inflammation, arteriosclerosis, and glomerulosclerosis.

Glomerulosclerosis and tubulointerstitial fibrosis are consequences of CKD progression secondary to an imbalance between excessive synthesis and reduced breakdown of the extracellular matrix replacing the renal cells [4]. The correlation of DTI parameters with CKD pathological subtypes was not studied before, it is needed to understand the types of structural changes and their effect on FA and ADC. In this study, FA of renal cortex/medulla was significantly different in patients with sclerotic CKD compared to non-sclerotic kidney disease. Deposition of the hyaline matrix in the renal cortex/medulla in sclerotic renal disease results in diffuse and nodular glomerulosclerosis, interstitial fibrosis, and tubular damage that will hinder the preferential diffusion of water molecules across the renal tubules in addition to blood stasis [23, 32]. This will result in reduced FA value in both the renal cortex/medulla as demonstrated by our results. ADC value also reduced in both the renal cortex/medulla despite being statistically insignificant likely due to a small number of the study population.

The renal medullary and cortical FA in patients with CKD are significantly correlated with serum creatinine and e-GFR in this study. Spearman's correlation was tested and resulted in a negative and positive correlation between the FA of the cortex/medulla and serum creatinine and e-GFR respectively. One study reported that there is a reducing trend in medullary FA values with higher stages of CKD [33]. However, others could not find this correlation in their study and attributed it to the marked heterogeneity of the study population [19]. Similar to our results, Saini et al. reported a negative correlation between FA of the renal medulla with serum creatinine ( $r=-0.785$ ) and a strong positive correlation between medullary FA with e-GFR in renal parenchymal disease ( $r=0.598$ ). In the current study, there was no significant correlation between renal cortical/medullary ADC with serum creatinine or GFR [34]. In a recent study, ADC extracted from intravoxel incoherent motion (IVIM) showed a positive correlation with e-GFR ( $r=0.72$ ) and a negative correlation with renal interstitial infiltrations ( $r=-0.44$ ) [35]. Moreover, Ren et al. reported a positive correlation between cortical ADC extracted from IVIM and e-GFR of the transplanted kidneys [36].

The first limitation of this study is the relatively small number of patients and control groups, further

multicentric studies including a larger number of pediatric CKD are recommended. Additionally, we could not assess the utility of DTI in differentiation between histopathological types of CKD. The second limitation was that DTI parameters were calculated through a uni-seed region of interest of the renal cortex/medulla. Multiparametric MR techniques such as intravoxel incoherent motion diffusion-weighted MRI (IVIM-DWI) with advanced post-processing methods such as histogram analysis in addition to artificial intelligence may improve the results since overall renal microstructural changes can be detected through more parameters.

## Conclusions

We concluded that renal cortical and medullary FA can help in the diagnosis of CKD and could predict sclerotic CKD. FA cortex/medulla correlate with some serum biomarkers.

## Abbreviations

DTI	Diffusion tensor imaging.
DWI	Diffusion-weighted imaging.
CKD	Chronic kidney disease.
FA	Fraction anisotropy.
ADC	Apparent diffusion coefficient.
KDIGO	Kidney Disease Improving Global Outcomes.
e-GFR	Estimated glomerular filtration rate

## Acknowledgements

Not applicable.

## Author contributions

All authors have read & approved the manuscript. Study concept and design were proposed by AAA, TB, and AH. Database search was done by MRA and MM. MM, AHE, and AAA helped in analysis and interpretation of imaging data. KMA and DAI contributed to analysis and interpretation of pathological data. MM, AHE, and MRA assisted in drafting of the manuscript. AHE, AH, and TB helped in revision of the manuscript. MRA and TB were involved in technical and clinical support.

## Funding

This study did not receive funding.

## Availability of data and materials

The authors declare that they had full access to all of the data in this study and the authors take complete responsibility for the integrity of the data and the accuracy of the data analysis.

## Declarations

### Ethics approval and consent to participate

A written informed consent was waived by Mansoura University institutional review board (IRB) as the study is meta-analysis.

### Consent for publication

Authors hereby transfer, assign, or otherwise convey all copyright ownership to the EJRN in the event that such work is published in that journal. Preprint is published in *authoria.com* (<https://doi.org/10.22541/au.161235171.19347933/v1>).

### Competing interests:

All authors disclosed no conflict of interest.



Received: 29 January 2024 Accepted: 2 April 2024  
Published online: 10 April 2024

## References

- Levin A, Stevens PE, Bilous RW et al (2013) Kidney disease: Improving Global Outcomes (KDIGO) CKD Work Group. KDIGO 2012 clinical practice guideline for the evaluation and management of chronic kidney disease. *Kidney Int Suppl* 3(1):1–150
- Becherucci F, Roperto RM, Materassi M et al (2014) Chronic kidney disease in children. *Clin Kidney J* 9:583–591
- Leaf IA, Duffield JS (2017) What can target kidney fibrosis? *Nephrol Dial Transplant* 32:i89–i97
- Nogueira A, Pires MJ, Oliveira PA (2017) Pathophysiological mechanisms of renal fibrosis: a review of animal models and therapeutic strategies. *In Vivo* 31:1–22
- Liu H, Zhou Z, Li X et al (2018) Diffusion-weighted imaging for staging chronic kidney disease: a meta-analysis. *BJR* 91:1091–20170952
- Caroli A, Schneider M, Friedli I et al (2018) Diffusion-weighted magnetic resonance imaging to assess diffuse renal pathology: a systematic review and statement paper. *Nephrol Dial Transplant* 33:ii29–ii40
- Elmokadem AH, Abdel Khalek AM, Abdel Wahab RM et al (2019) Diagnostic accuracy of multiparametric magnetic resonance imaging for differentiation between parotid neoplasms. *Can Assoc Radiol J* 70(3):264–272
- Saleh GA, Alghandour R, Rashad EY et al (2021) The adjunctive value of diffusion weighted imaging in diagnosis and follow up of uterovaginal diffuse B-cell lymphoma: a case report and literature review. *Curr Med Imaging* 17(9):1159–1166
- Razek AA, Khashaba M, Abdalla A et al (2014) Apparent diffusion coefficient value of hepatic fibrosis and inflammation in children with chronic hepatitis. *Radiol Med* 119:903–909
- Saleh GA, Elmokadem AH, Razek AA et al (2023) Utility of diffusion tensor imaging in differentiating benign from malignant hepatic focal lesions. *Eur Radiol* 33(2):1400–1411
- Sherif F, Elmokadem AH, Abdel Razek A et al (2022) DTI of the olfactory bulb in COVID-19-related anosmia: a pilot study. *AJNR* 43:1180–1183
- Zheng Z, Shi H, Zhang J et al (2014) Renal water molecular diffusion characteristics in healthy native kidneys: assessment with diffusion tensor MR imaging. *PLoS ONE* 9:e113469
- Fan W, Ren T, Li Q et al (2016) Assessment of renal allograft function early after transplantation with isotropic resolution diffusion tensor imaging. *Eur J Radiol* 26:567–575
- Palmucci S, Cappello G, Attina G et al (2015) Diffusion weighted imaging and diffusion tensor imaging in the evaluation of transplanted kidneys. *Eur Radiol* 2:71–80
- Nassar MK, Khedr D, Abu-Elfadl HG et al (2015) Diffusion Tensor Imaging in early prediction of renal fibrosis in patients with renal disease: Functional and histopathological correlations. *Int J Clin Pract* 75(4):e13918
- Zhao J, Wang Z, Liu M et al (2014) Assessment of renal fibrosis in chronic kidney disease using diffusion-weighted MRI. *Clin Radiol* 69:1117–1122
- Feng Q, Ma Z, Wu J, Fang W (2015) DTI for the assessment of disease stage in patients with glomerulonephritis—correlation with renal histology. *Eur Radiol* 25:92–98
- Liu Z, Xu Y, Zhang J et al (2015) Chronic kidney disease: pathological and functional assessment with diffusion tensor imaging at 3T MR. *Eur Radiol* 25:652–660
- Gaudio C, Clementi V, Busato F et al (2013) Diffusion tensor imaging and tractography of the kidneys: assessment of chronic parenchymal diseases. *Eur Radiol* 23:1678–1685
- Razek AA, Khalek AM, Tharwat S et al (2021) Diffusion tensor imaging of renal cortex in lupus nephritis. *Jpn J Radiol* 39:1069–1076
- Cakmak P, Yağcı AB, Dursun B et al (2014) Renal diffusion-weighted imaging in diabetic nephropathy: correlation with clinical stages of disease. *Diagn Interv Radiol* 20:374–378
- Lu L, Sedor JR, Gulani V et al (2011) Use of diffusion tensor MRI to identify early changes in diabetic nephropathy. *Am J Nephrol* 34:476–482
- Hueper K, Hartung D, Gutberlet M et al (2012) Magnetic resonance diffusion tensor imaging for evaluation of histopathological changes in a rat model of diabetic nephropathy. *Invest Radiol* 47:430–437
- Pottel H, Dubourg L, Goffin K et al (2018) Alternatives for the bedside Schwartz equation to estimate glomerular filtration rate in children. *Adv Chronic Kidney Dis* 25:57–66
- Özkana MB, Marterer R, Tscheunerb S et al (2016) The role of kidney diffusion tensor magnetic resonance imaging in children. *EJRN* 47:1599–1611
- Simrén Y, Stokland E, Hansson S et al (2021) Diffusion tensor imaging based multiparametric characterization of renal lesions in infants with urinary tract infections: an explorative study. *BMC Pediatr* 21(1):440
- Donnola SB, Piccone CM, Lu L et al (2018) Diffusion tensor imaging MRI of sickle cell kidney disease: initial results and comparison with iron deposition. *NMR Biomed*. <https://doi.org/10.1002/nbm.3883>
- Li Y, Lee MM, Worters PW et al (2017) Pilot study of renal diffusion tensor imaging as a correlate to histopathology in pediatric renal allografts. *AJR Am J Roentgenol* 208(6):1358–1364
- Ye XJ, Cui SH, Song JW et al (2019) Using magnetic resonance diffusion tensor imaging to evaluate renal function changes in diabetic patients with early-stage chronic kidney disease. *Clin Radiol* 74(2):116–122
- Hueper K, Gutberlet M, Rodt T et al (2011) Diffusion tensor imaging and tractography for assessment of renal allograft dysfunction—initial results. *Eur Radiol* 21:2427–2433
- Mao W, Zhou J, Zeng M et al (2018) Chronic kidney disease: Pathological and functional evaluation with intravoxel incoherent motion diffusion-weighted imaging. *J Magn Reson Imaging* 47:1251–1259
- Thoeny HC, De Keyser F, Oyen RH et al (2005) Diffusion-weighted MR imaging of kidneys in healthy volunteers and patients with parenchymal diseases: initial experience. *Radiology* 235:911–917
- Berchtold L, Friedli I, Vallée JP et al (2017) Diagnosis and assessment of renal fibrosis: the state of the art. *Swiss Med Wkly* 147:w14442
- Saini S, Kumar V, Koteshwara P (2018) Role of diffusion tensor imaging in renal parenchymal changes. *Indian J Radiol Imaging* 28:175–181
- Sulkowska K, Palczewski P, Furmańczyk-Zawiska A et al (2020) Diffusion weighted magnetic resonance imaging in the assessment of renal function and parenchymal changes in chronic kidney disease: a preliminary study. *Ann Transplant* 25:e920232
- Ren T, Wen CL, Chen LH et al (2016) Evaluation of renal allografts function early after transplantation using intravoxel incoherent motion and arterial spin labeling MRI. *Magn Reson Imaging* 34:908–914

## Publisher's Note

Springer Nature remains neutral with regard to jurisdictional claims in published maps and institutional affiliations.